

M. BIELNICKI\*, J. JOWSA\*, A. CWUDZIŃSKI\*

## MULTIPHASE NUMERICAL MODEL OF MOLTEN STEEL AND SLAG BEHAVIOR IN THE CONTINUOUS CASTING MOULD

### WIELOFAZOWY MODEL NUMERYCZNY ZACHOWANIA SIĘ CIEKŁEJ STALI I ŻUŻŁA W KRYSZALIZATORZE COS

The paper reports the results of numerical simulation of the flow of liquid steel with the use of a multiphase model. The facility under study was a mould designed for continuous casting of steel slabs. The geometry of the facility, along with the computational grid, was generated within the program Ansys-Meshing<sup>®</sup>. Numerical computations were performed in the programs: COMSOL Multiphysics<sup>®</sup> and Ansys-Fluent<sup>®</sup>. The use of the multiphase model enabled the determination of the behavior of the liquid slag layer on the metal bath surface. From the performed computer simulations, the fields of liquid steel motion and liquid steel turbulence kinetic energy distribution in the mould's symmetry plane have been presented. Based on the values recorded at selected measurement points located on the slag surface, a diagram illustrating the variation of the slag layer position during continuous steel casting has been plotted.

*Keywords:* continuous casting mould, liquid steel, slag, multiphase fluid flow model

W niniejszej pracy przedstawiono wyniki symulacji numerycznej przepływu ciekłej stali z wykorzystaniem modelu wielofazowego. Badanym obiektem był krystalizator przeznaczony do ciągłego odlewania stalowych wlewków płaskich. Geometrię obiektu wraz z siatką obliczeniową wygenerowano w programie Ansys-Meshing<sup>®</sup>. Obliczenia numeryczne wykonano w programach: COMSOL Multiphysics<sup>®</sup> i Ansys-Fluent<sup>®</sup>. Zastosowanie modelu wielofazowego pozwoliło na określenie zachowania się warstwy ciekłego żużła na powierzchni kąpieli metalowej. Na podstawie wykonanych symulacji komputerowych zaprezentowano pola ruchu ciekłej stali oraz rozkładu kinetycznej energii turbulencji ciekłej stali w płaszczyźnie symetrii krystalizatora. Bazując na wartościach zarejestrowanych w wybranych punktach pomiarowych, znajdujących się na powierzchni żużła, sporządzono wykres obrazujący zmianę położenia warstwy żużła podczas ciągłego odlewania stali.

### 1. Introduction

In the process of continuous steel casting, the liquid metal is transferred from the ladle to the tundish and then, through the submerged entry nozzle (SEN), to the mould. The heat removal from the metal bath through the mould water cooling system allows a solidified shell layer to be formed [1]. At the same time, during the course of the process, mould powder is added to the surface of the liquid metal in the mould. The mould powder performs many important functions having a significant influence on the mould operation conditions and the final quality of produced slab, bloom and billet. It protects the liquid steel against re-oxidation. In addition, it acts as an insulator protecting the metal bath against excessive heat losses from the steel surface and absorbs non-metallic inclusions and impurities. Part of the powder gets melted to create a thin layer of liquid slag that covers the steel surface and fills the gap formed between the mould walls and the solidified layer of slab being formed. The liquid slag has the effect of reducing the friction coefficient between the solidified shell and the mould wall and determines the surface quality of the cast slab (e.g. the magnitude and geometry of the oscillation

marks) [2]. Moreover, it enables the heat exchange coefficient adjusted to the assumed casting conditions and the cast steel grade to be achieved.

The dynamic interaction of the liquid steel with the liquid slag determines the shape and geometry of the contact surface and the variation of the thickness of the slag and powder layers, which also significantly influences the quality of the finished product [3]. Excessive surface fluctuations in the region of contact between two phases may lead to the adverse phenomenon of carrying mould powder particles away into the metal bath. Based on the investigations [4, 5], attention was drawn to some mechanisms responsible for this phenomenon, namely: the backflow (the rebound of the steel stream flowing out from the submerged entry nozzle ports from the narrower mould walls), the shearing stresses created by backflow oscillations, the interaction of argon bubbles with the mould powder layer, the pressure drops in the vicinity of the submerged entry nozzle caused by the oscillatory behavior of the backflow.

The mould powder entrainment is, therefore, a serious problem during casting slabs, blooms and billets by the continuous method. The examination of this phenomenon under

\* CZĘSTOCHOWA UNIVERSITY OF TECHNOLOGY, DEPARTMENT OF METALS EXTRACTION AND RECIRCULATION, FACULTY OF PRODUCTION ENGINEERING AND MATERIALS TECHNOLOGY, 19 ARMII KRAJOWEJ AV., 42-200 CZĘSTOCHOWA, POLAND

industrial conditions faces great difficulties (due to the high temperature, the lack of transparency of all phases), therefore alternative methods are being developed to enable the understanding of the fundamental physical phenomena occurring in the area of the forming meniscus. To this end, water models [6, 7], laboratory models relying on low-melting point alloys [8], or numerical modelling using appropriate mathematical descriptions are employed [8, 9].

## 2. Description of the test facility

The facility under study was a mould designed for continuous casting of steel slabs. The facility is equipped with a submerged entry nozzle with two lateral discharge ports inclined downwards at an angle of  $7^\circ$  in relation to the SEN cross-section. The inner diameter of the SEN is 65 mm. The SEN ports have the shape of a  $60 \times 100$  mm rectangular with a rounded corners (a rounding radius of 10 mm). The internal geometry of the SEN below the ports is concave. The immersion depth of the SEN is 150 mm. The examined mould enables  $0.225 \times 1.6$  m slabs to be cast. Fig. 1 shows a fragment of the cross-section of the discharge system, located in the upper mould zone, and the prepared computational grid.

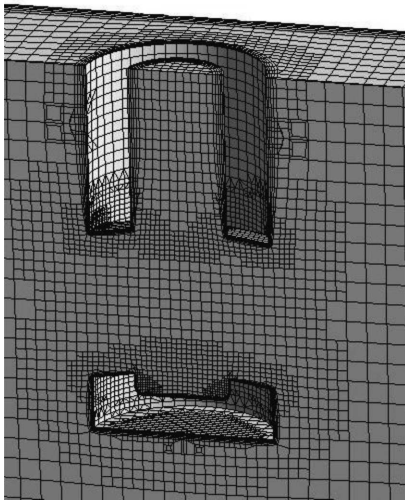


Fig. 1. Scheme of test facility with the computational grid

## 3. Description of the mathematical models

Level Set [10], Phase Field [11] and Volume of Fluid (VOF) [12] method are well-known interface capturing techniques for calculation of moving interfaces in multiphase systems. These methods compute two-phase or multiphase flow on fixed Eulerian grid.

In method Level Set the interface is represented by a certain level set of a globally defined function – the level set function  $\phi$ . Across the interface there is smooth transition from zero to one. The interface is defined by the 0.5 contour of  $\phi$ . Model Level set solves the following equation in order to move the interface with velocity  $v$ :

$$\frac{\partial \phi}{\partial t} + \mathbf{u} \nabla \phi = \gamma \nabla \cdot \left( \varepsilon \nabla \phi - \phi (1 - \phi) \frac{\nabla \phi}{|\nabla \phi|} \right) \quad (1)$$

with of the Navier-Stokes equations:

$$\rho \frac{\partial \mathbf{u}}{\partial t} + \rho (\mathbf{u} \cdot \nabla) \mathbf{u} = \nabla \cdot \left[ -p \mathbf{I} + \mu (\nabla \mathbf{u} + \nabla \mathbf{u}^T) \right] + \mathbf{F}_g + \mathbf{F}_{st} \quad (2)$$

$$\nabla \cdot \mathbf{u} = 0 \quad (3)$$

where:  $\varepsilon$  – parameter determines the thickness of the region where  $\phi$  goes smoothly from zero to one,  $\gamma$  – parameter determines stabilization of the level set function,  $\mathbf{u}$  – overall velocity vector,  $t$  – time,  $\nabla$  – nabla operator,  $p$  – pressure,  $\mathbf{I}$  – identity matrix,  $\mathbf{F}_g = \rho \mathbf{g}$  – gravity force where  $\mathbf{g}$  is the gravity vector,  $\mathbf{F}_{st} = \sigma \kappa \delta \mathbf{n}$  – surface tension force acting on interface between the two fluids, where  $\sigma$  – is the surface tension coefficient,  $\kappa$  is the curvature,  $\delta$  is a Dirac delta function located at the interface and  $\mathbf{n} = \frac{\nabla \phi}{|\nabla \phi|}$  is the unit normal to interface.

The density and the dynamic viscosity are a function of the level set function defined as:

$$\rho = \rho_1 + (\rho_2 - \rho_1) \phi \quad (4)$$

$$\mu = \mu_1 + (\mu_2 - \mu_1) \phi \quad (5)$$

where:  $\rho_1$  and  $\rho_2$  are the densities of steel and slag, respectively, and  $\mu_1$  and  $\mu_2$  are the dynamic viscosities of steel and slag, respectively.

Phase Field method is based on physical approach which incorporates the phases and interface between them into the free energy function of the system. It mean that Phase Field method not only transports the interface with the flow, but ensures that the total energy of system is minimized correctly. If the Phase Field method is used to track the interface, it adds to the Navier-Stokes the following equations:

$$\frac{\partial \phi}{\partial t} + \mathbf{u} \cdot \nabla \phi = \nabla \cdot \frac{\gamma \lambda}{\varepsilon^2} \nabla \psi \quad (6)$$

$$\psi = -\nabla \cdot \varepsilon^2 \nabla \phi + (\phi^2 - 1) \phi \quad (7)$$

where:  $\lambda$  is the quantity of the mixing energy density,  $\varepsilon$  is capillary width that scales with the thickness of the interface. These two parameters are related to the surface tension coefficient through equation:

$$\sigma = \frac{2\sqrt{2}\lambda}{3\varepsilon} \quad (8)$$

Parameter  $\gamma$  in equation (6) is related to  $\varepsilon$  through  $\gamma = \chi \varepsilon^2$  where  $\chi$  is the mobility tuning parameter. The density and the dynamic viscosity are defined as:

$$\rho = \rho_1 + (\rho_2 - \rho_1) V_f \quad (9)$$

$$\mu = \mu_1 + (\mu_2 - \mu_1) V_f \quad (10)$$

where:  $V_f$  – volume fraction is computed as

$$V_f = \min(\max([(1 + \phi)/2], 0), 1) \quad (11)$$

where the **min** and **max** operators are used so that the volume fraction has a lower limit of 0 and an upper limit of 1.

The surface tension force for the Phase Field method is computed as

$$\mathbf{F}_{st} = G \nabla \phi \quad (12)$$

where  $G$  is the chemical potential defined as

$$G = \lambda \left[ -\nabla^2 \phi + \frac{\phi(\phi^2 - 1)}{\varepsilon^2} \right] \quad (13)$$

The most popular methods to front tracking is VOF method. This method originally introduced by Hirt and Nichols [12] implicitly tracks interfaces through the volume fraction function. Each cell is assigned a volume fraction ( $\alpha_p, \alpha_q$ ) between zero to one to indicate the averaged relative amount of one of the fluids. A cell with a volume fraction of zero or one will be completely filled with either of the fluids, while a cell with an intermediate volume fraction will have an interface segment intersecting it. The main advantage of the VOF method is that it conserves mass accurately even for a coarse numerical grid. The density ( $\rho$ ) and viscosity ( $\mu$ ) in each cell at interface were computed by the application of following equations:

$$\rho = \alpha_q \rho_q + (1 - \alpha_q) \rho_p \quad (14)$$

$$\mu = \alpha_q \mu_q + (1 - \alpha_q) \mu_p \quad (15)$$

where:  $\alpha_q$  – volume fraction of phase q,  $\rho_p$  – density of phase p,  $\rho_q$  – density of phase q,  $\mu_p$  – viscosity of phase p,  $\mu_q$  – viscosity of phase q.

The tracking of the interfaces between the phases is accomplished by the solution of a continuity equation for the volume fraction of one of the phases (or more phases). For the  $q^{th}$  phase, this equation has the following form:

$$\frac{1}{\rho_q} \left[ \frac{\partial}{\partial t} (\alpha_q \rho_q) + \nabla \cdot (\alpha_q \rho_q \mathbf{u}) = \sum_{p=1}^n (\dot{m}_{pq} - \dot{m}_{qp}) \right] \quad (16)$$

where:  $\dot{m}_{qp}$  – is the mass transfer from phase q to phase p,  $\dot{m}_{pq}$  – is the mass transfer from phase p to phase q.

The momentum equation has form equations (2). The surface tension force for VOF method has the following form:

$$\mathbf{F}_{st} = \sum_{pairs} \sum_{i,j} \sum_{i < j} \sigma_{ij} \frac{\alpha_i \rho_i \kappa_j \nabla \alpha_j + \alpha_j \rho_j \kappa_i \nabla \alpha_i}{\frac{1}{2} (\rho_i + \rho_j)} \quad (17)$$

The curvature ( $\kappa$ ) is defined in terms of the divergence of unit normal ( $\mathbf{n}$ )

$$\kappa = \nabla \cdot \mathbf{n} \quad (18)$$

The tracking of the interface is accomplished by an implicit scheme, which solves the face fluxes ( $\dot{m}$ ) in each grid cell through equation:

$$\frac{\alpha_q^{n+1} \rho_q^{n+1} - \alpha_q^n \rho_q^n}{\Delta t} V + \sum_f (\rho_q^{n+1} U_f^{n+1} \alpha_{q,f}^{n+1}) = \left[ \sum_{p=1}^n (\dot{m}_{pq} - \dot{m}_{qp}) \right] V \quad (19)$$

where:  $V$  – volume of cell,  $U_f$  – volume flux through the face,  $\alpha_{q,f}$  – face value of the  $q^{th}$  volume fraction,  $^{n+1}$  – index for new time step,  $^n$  – index for previous time step.

#### 4. Conditions of conducting numerical simulations

Due to the time-consuming nature of the numerical computation of the behaviour of steel and slag in the mould, preliminary studies were carried out for a two-dimensional model,

and since the facility is symmetrical, half of the facility was taken for the studies. Moreover, an additional simplification was adopted by assuming that the upper slag surface was plane with zero tangential stresses. Whereas, the proper studies were conducted for the three-dimensional system, allowing for the free formation of the upper liquid slag surface in contact with the gaseous phase. Hence, the system under examination is indeed a three-phase system.

The following physicochemical properties of individual system phases were assumed in numerical simulation: liquid steel density: 7010 kg/m<sup>3</sup>; liquid slag density: 2600 kg/m<sup>3</sup>; air density: 1.225 kg/m<sup>3</sup>; liquid steel viscosity: 0.007 Pa·s; liquid slag viscosity: 0.14 Pa·s; interfacial tension liquid steel-liquid slag: 0.12 N/m; interfacial tension liquid steel-air: 1.6 N/m. It was determined that the thickness of the liquid slag layer for the model 3D was 0.03 m.

Computations were performed for isothermal conditions, in a transient state, with a time step of 0.1 s. The solution of the equations was considered convergent, if the values of all residues fell below the value 10<sup>-3</sup>. In order to monitor the variations in the shape of the slag phase profile, before starting the computation, three virtual measurement points were positioned on the slag surface, located at a distance of 0.2; 0.4 and 0.75 m from the system's axis of symmetry (the SEN axis).

The three-dimensional representation of the examined facility was made in the program Gambit. The computational grid, made up of 658 thousand cubic elements, was generated in the program Ansys-Meshing<sup>®</sup>. To obtain more precise results of the interaction of the contacting system phases, the computational grid was adaptively densified in the slag phase occurrence region and in the regions 1 cm above and below the slag layer in the program Ansys-Fluent<sup>®</sup>. The flow of liquid steel in the mould was simulated in the program Ansys-Fluent<sup>®</sup>. The following boundary conditions were assigned to the virtual mould model: velocity inlet – on the SEN cross-section, outflow – on the wall representing the lower mould surface, slip-wall – for the upper model plane, no-slip-wall – for the remaining planes of the facility. To describe the coupling of the pressure and velocity fields, the SIMPLEC algorithm was used. The pressure field was solved using the PRESTO! method. As the steel flow in the mould is dynamic, the turbulence of this motion was described with a two-equation model of the Realizable k- $\varepsilon$  type [13].

At the mould inlet, the following boundary conditions were assumed: liquid steel velocity: 1.3 m/s; turbulent kinetic energy: 0.0169 m<sup>2</sup>/s<sup>2</sup>, turbulent dissipation rate: 0.06277 m<sup>2</sup>/s<sup>3</sup>.

#### 5. Results

To carry out simulation (2D) of the casting of steel covered with a slag layer in the mould, the two previously discussed methods, i.e. Phase Field and Level Set, were employed. The results representing the formation of the interface indicate, that a wave travels along the metal surface, which is more intensive at the initial steel pouring moment, and lowers its crest as the casting time passes. Finally, the shape of the surface is similar to the one in Fig. 2. In the region at the

side mould wall the steel surface is elevated compared to the initial state. This is caused by the circulatory motion of the upper vortex. Similar pictures of the steel-slag interface state were obtained for the both of the employed methods, when the measurement duration did not exceed 5s. After that time, the picture acquired by the Level Set method substantially changed, as larger and smaller slag particles started to appear in the mould region filled with liquid steel. An example of this state is illustrated in Fig. 3.

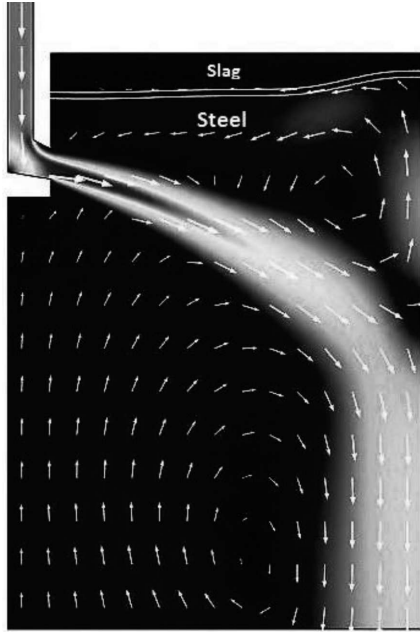


Fig. 2. The picture of the liquid steel and slag interaction state recorded by the Phase Field method after a time of 10s

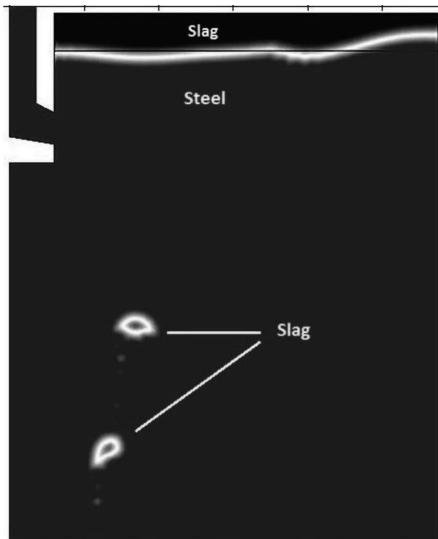


Fig. 3. The picture of the liquid steel and slag interaction state recorded by the Level Set method after a time of 10s

At that stage it was difficult to judge what could be the causes of this phenomenon, as they might have been seen in the properties and the difference between the employed computational methods, or this could have been the natural effect of "taking away" and absorbing the slag and the powder by the liquid steel. So, it was decided to check what interaction

effect would be on the 3D object, assuming the upper slag surface was freely formed by the metal waves caused by the steel flowing out from the SEN ports. For this purpose, the Volume of Fluid model was used, which had proved itself in many applications, e.g. for determining the boundaries of the solidified slab in the continuous casting process.

Based on performed computations, the fields of liquid steel motion in the mould working space, turbulence kinetic energy values and slag layer shape variation during the course of the process were obtained.

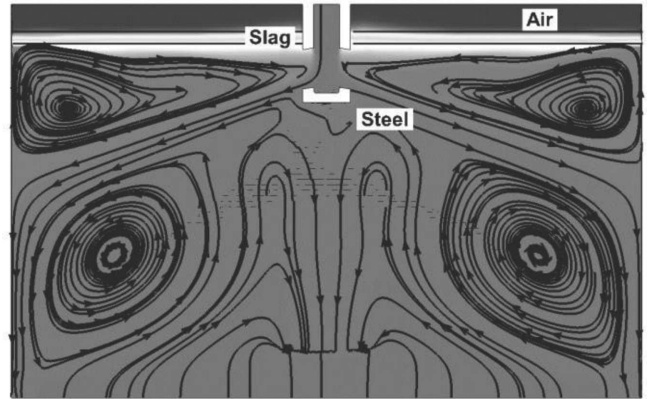


Fig. 4. Velocity streamlines of liquid steel in the symmetry plane of the mould

Fig. 4 represents current lines in the liquid steel after 108 seconds from the moment of starting the casting process. The indicated slag layer thickness relates to the state prior to starting the simulation. The obtained flow pattern is characteristic of continuous slab casting moulds equipped with a submerged entry nozzle with two lateral ports oriented downwards relative to the SEN cross-section. In the figure, a slight flow asymmetry can be observed. The liquid steel flow is made up of four recirculation zones, similarly as in the 2D object. The metal stream flows out from the lateral ports and moves towards the narrower mould walls. After "hitting" against the narrower mould wall, it becomes deflected to form two separate streams. One of those streams moves along the narrower mould wall towards the meniscus. After reaching the meniscus surface, it gets deflected again and then moves along the slag layer towards the SEN. The other stream moves down the mould along its narrower wall. Near the lower edge of the facility, it is deflected and, in the form of backflow, heads back for the lateral ports of SEN.

The distribution of liquid steel velocity in the vicinity of the meniscus influences its shape and the behavior of the slag layer. In order to explain the effect of steel motion on the slag surface oscillations in the sub-meniscus zone, liquid steel velocity values were read out along the line located 0.01 m below the meniscus level (Fig. 5).

Computations showed that the distribution of velocity values in the sub-meniscus zone is not uniform. The difference in magnitudes and senses between liquid steel velocity vectors in different sub-meniscus zone regions results in a distortion of the meniscus of the metal bath and the slag layer. The largest velocity magnitudes were found in the vicinity of the narrower mould walls (0.1 m/s). This is caused by the effect of the upper steel vortex along the narrower mould wall towards



the meniscus. This flow causes an elevation of the metal level near the narrower mould wall and a lowering of the slag layer in the SEN zone.

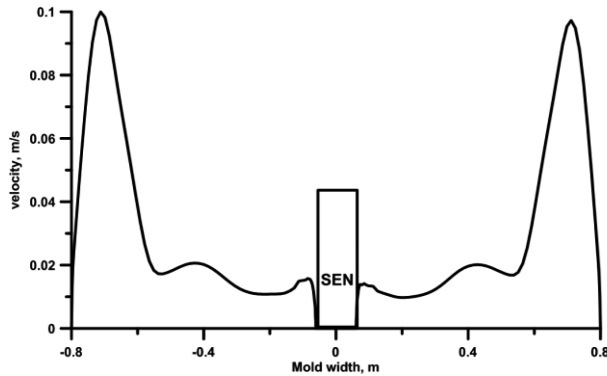


Fig. 5. Values of liquid steel velocity along the horizontal line located at the distance 0.01 m below meniscus level

The risk of occurring the adverse phenomenon of "carrying away" the slag layer into the metal bath depends, inter alia, on the difference in kinematic viscosity between the liquid steel and the slag, the difference in density between the metal bath and the slag and the interface tension between them [5]. Based on the results of study [14] it has been found that for the phenomenon of slag entrainment by the metal bath to occur, the velocity of liquid steel motion in the sub-meniscus zone must exceed the value of 0.2 m/s. In the situation under discussion, the maximum velocity of liquid steel motion below the meniscus level was 0.1 m/s, so there is no real risk of powder entrainment. Therefore, the slag entrainment computation results obtained in the 2D model using the Level Set method are probably incorrect, though they may not be totally rejected without carrying out additional studies.

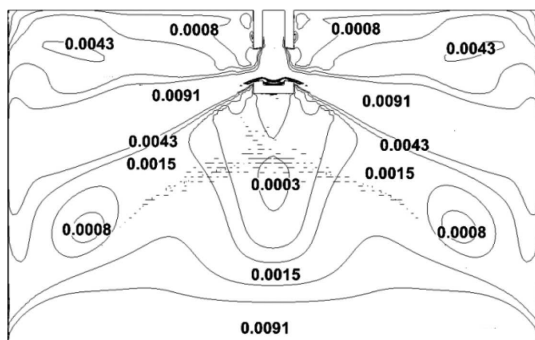


Fig. 6. The distribution of turbulence kinetic energy ( $\text{m}^2/\text{s}^2$ ) in the symmetry plane of the mould

Fig. 6 illustrates the distribution of turbulence kinetic energy in the symmetry plane of the examined mould. The computed values are characterized by the complete symmetry relative to the SEN axis. The largest values of turbulence kinetic energy were observed in the region of the liquid steel stream flowing out from the SEN lateral ports and in the lower part of the mould, where the kinetic energy was  $0.0091 \text{ m}^2/\text{s}^2$ . The smallest values,  $0.0008 \text{ m}^2/\text{s}^2$ , were recorded in the sub-meniscus zone in the vicinity of the SEN and in the central regions of the lower recirculation zones. The computations have also shown that the central regions of the upper recirculation zones are distinguished by much larger values

of turbulence kinetic energy compared to the regions of the lower recirculation zones.

Very noteworthy is the picture of slag layer waving obtained from numerical simulations properly carried out. Fig. 7 displays curves representing variations in the slag level during casting. It was assumed that the measurement would be taken at three points lying in the vertical plane passing through the axis of the SEN at a distance of  $x = 0.2 \text{ m}$ ;  $0.4 \text{ m}$  and  $0.75 \text{ m}$  from the SEN axis. The curves suggest the motion of the liquid slag due to the interaction with the liquid steel. It was assumed in the simulation that the initial slag layer height was  $0.03 \text{ m}$ . The main cause of the different values recorded in time  $t = 0$  was probably the use of too large time step at the initial simulation stage. At the measurement point with the coordinate  $x = 0.75 \text{ m}$ , the highest slag layer level was found (both at the initial and final simulation stages). The high slag layer level in this region of the mould was caused by the liquid steel flow of a relatively high velocity ( $0.1 \text{ m/s}$ ) along the narrower mould wall towards the meniscus, which resulted in a rise of the metal bath level in this region and, as a consequence, an elevation of the liquid slag level. This state is confirmed by the results of computation on the 2D model for the both of the employed numerical methods. Simulations conducted for a time period more than 100s did not reveal any precipitation of the slag phase in the three-dimensional mould region.

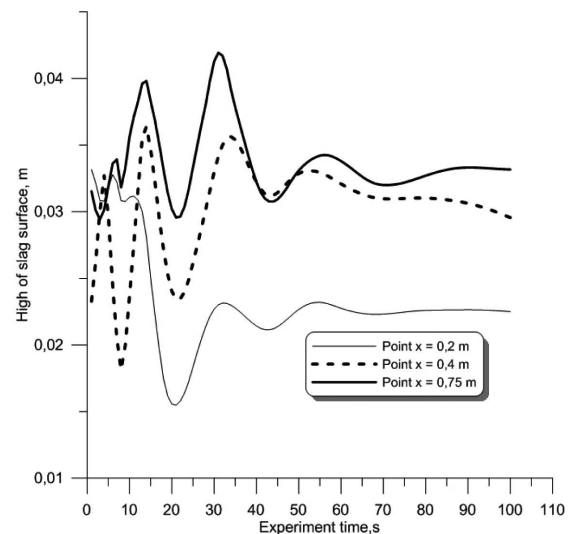


Fig. 7. Variation in slag surface height at three monitoring points

## 6. Conclusions

Based on the numerical simulations of steel flow in the mould with a submerged entry nozzle, the following has been determined:

- the VOF multiphase model enables the variations in the liquid slag level to be determined during the course of the continuous steel casting process,
- the distribution of metal bath motion within the mould working volume causes a rise in the liquid steel layer in the vicinity of the narrower mould walls; also, the largest steel motion values in the sub-meniscus zone were observed near the narrower mould walls,

- the greatest turbulence kinetic energy values were noted in the region of the liquid metal stream flowing out from the lateral SEN ports and in the lower part of the mould. The values of turbulence kinetic energy in plane of symmetry of the examined facility are symmetrical with respect of the SEN,
- the recorded variations in slag layer height differed, depending on the location of the monitoring point. The highest liquid slag level was observed near the narrower mould wall, while the lowest – in the vicinity of SEN,
- with the existing conditions of continuous slab casting, the condition of drawing in the slag and the powder to the liquid steel filling the mould seems very little probable.

#### REFERENCES

- [1] Z. Malinowski, T. Telejko, B. Haduła, *Archiv. of Metal. Mater.* **57**, 325 (2012).
- [2] H. Kania, J. Gawor, *Archiv. of Metal. Mater.* **57**, 339 (2012).
- [3] A. Sorek, Z. Kudliński, *Archiv. of Metal. Mater.* **57**, 371 (2012).
- [4] S. Yamashita, M. Iguchi, *ISIJ Int.* **41**, 1529 (2001).
- [5] M. Iguchi, J. Yoshida, T. Shimizu, Y. Mizuno, *ISIJ Int.* **40**, 685 (2000).
- [6] P.R. Scheller, R. Hagemann, *Archiv. of Metal. and Mater.* **57**, 283 (2012).
- [7] Y.J. Jeon, H.J. Sung, S. Lee, *Metall. and Material. Trans. B* **41B**, 121 (2010).
- [8] P.E. Ramirez-Lopez, P.N. Jalali, J. Björkvall, U. Sjöström, C. Nilsson, *ISIJ Int.* **54**, 342 (2014).
- [9] J. Calderon-Ramos, J. de J. Barreto, S. Garcia-Hernandez, *ISIJ Int.* **53**, 802 (2013).
- [10] S. Osher, J.A. Setian, *J. Comput. Phys.* **79**, 12 (1988).
- [11] D. Jacqmin, *J. Comput. Phys.* **155**, 96 (1999).
- [12] C.W. Hirt, B.D. Nichols, *J. Comput. Phys.* **39**, 201 (1981).
- [13] A. Cwudziński, *Metall. Res. Technology* **111**, 45 (2014).
- [14] P.R. Cha, J.K. Yoon, *Metall. and Material. Trans. B* **31B**, 317 (2000).